

# Electrical breakdown and ultrahigh electrical energy density in poly(vinylidene fluoride-hexafluoropropylene) copolymer

Xin Zhou,<sup>1</sup> Xuanhe Zhao,<sup>2</sup> Zhigang Suo,<sup>2</sup> Chen Zou,<sup>3</sup> James Runt,<sup>4</sup> Sheng Liu,<sup>1</sup> Shihai Zhang,<sup>5</sup> and Q. M. Zhang<sup>1,3,a)</sup>

<sup>1</sup>Department of Electrical Engineering, The Pennsylvania State University, University Park, Pennsylvania 16802, USA

<sup>2</sup>School of Engineering and Applied Science, Harvard University, Cambridge, Massachusetts 02138, USA

<sup>3</sup>Materials Research Institute, The Pennsylvania State University, University Park, Pennsylvania 16802, USA

<sup>4</sup>Department of Materials Science and Engineering, The Pennsylvania State University, University Park, Pennsylvania 16802, USA

<sup>5</sup>Strategic Polymer Science, Inc., State College, Pennsylvania 16803, USA

(Received 2 March 2009; accepted 31 March 2009; published online 20 April 2009)

This paper investigates the electrical breakdown of a polar fluoropolymer, poly(vinylidene fluoride-hexafluoropropylene) which exhibits an exceptionally high discharged electrical energy density ( $>25 \text{ J/cm}^3$ ). It is shown that above room temperature, the breakdown strength decreases with temperature. It is further shown that such a temperature dependence of breakdown strength is consistent with the electromechanical breakdown model by taking into consideration of the plastic deformation of semicrystalline polymers. © 2009 American Institute of Physics.  
[DOI: 10.1063/1.3123001]

Dielectric materials with high energy storage density are of great importance for the power electronics in hybrid electric vehicles, medical devices, and electrical weapon systems.<sup>1,2</sup> Among various dielectric materials, polymers are presently the material choice for high energy density capacitors because of the combination of high breakdown strength, low cost, and graceful failure nature.<sup>3,4</sup> Recently, we reported that in polar fluoropolymers, by properly tuning the dielectric constant to avoid the electrical displacement saturation at electrical fields far below the breakdown field, a very high electrical energy density ( $>17 \text{ J/cm}^3$ ) can be achieved in a poly(vinylidene fluoride-chlorotrifluoroethylene) [P(VDF-CTFE)] copolymer.<sup>5,6</sup>

In this paper, we show that by improving the film processing conditions and consequently the film quality, a higher electrical breakdown field can be achieved in another polar fluoropolymer, poly(vinylidene fluoride-hexafluoropropylene) [P(VDF-HFP)], which leads to the electrical energy density higher than  $25 \text{ J/cm}^3$  at room temperature. Since the energy density is closely associated with the electrical breakdown field, we examined the electrical breakdown mechanism in this class of polar fluoropolymers. It is observed that above room temperature the breakdown strength decreases with temperature, suggesting that the electromechanical breakdown is responsible for the dielectric failure at high field due to the reduction in elastic modulus with temperature.<sup>7-11</sup> Comparing the observed results with the widely used Stark-Garton electromechanical breakdown model reveals that the model greatly overestimates the breakdown field.<sup>7-11</sup> To correct for that, we introduce a general power law model to include the plastic deformation for semicrystalline polymers and show that the predicted electromechanical breakdown strength of the new model agrees quite well with the experimental data.

P(VDF-HFP) 95.5/4.5 mol % random copolymer used in this study was purchased from Solvay. The films were prepared by an extrusion process, a standard polymer capacitor film production method. This method reduces the contaminations of the films from environmental dusts (defects), compared with the small scale film fabrication method used in the earlier publication, and improves the breakdown fields.<sup>5,6</sup> A zone drawing machine was used to uniaxially stretch the films to five times of their original length at  $110 \text{ }^\circ\text{C}$ , which also improves the breakdown fields. The thickness of the stretched films is between 3 and  $11 \text{ } \mu\text{m}$ . Aluminum electrodes of 3.18 mm diameter and 40 nm thickness were thermally deposited under high vacuum. dc breakdown tests on P(VDF-HFP) films were performed using a voltage ramp rate of 500 V/s. The breakdown field as a function of temperature and thickness was investigated and under each condition, at least 30 measurements were made. The breakdown strength of the dielectric films was evaluated by the two-parameter Weibull analysis,<sup>12</sup>

$$P(E) = 1 - \exp[-(E/E_b)^\beta], \quad (1)$$

where  $E$  is the measured electrical breakdown strength,  $E_b$  is the characteristic breakdown field, and  $\beta$  is a shape parameter. The discharged energy density was measured by a Sawyer-Tower circuit at a frequency of 10 Hz. The Young's modulus of the films was characterized by a dynamic mechanical analyzer (TA Instrument, DMA2980). The dielectric constant was acquired by a LCR meter (HP 4284A) equipped with a computer controlled temperature chamber. The stress-strain curves of the films were measured by an Instron machine (Model 5866).

Figure 1(a) presents the discharged electric energy density  $U_r$  at room temperature and an  $U_r > 25 \text{ J/cm}^3$  at 700 MV/m can be achieved, which represents one order of magnitude improvement over the widely used state-of-the-art biaxially oriented polypropylene capacitor films and other dielectric films.<sup>1,3</sup> The high energy density of this copolymer is

<sup>a)</sup>Electronic mail: qxzl@psu.edu.

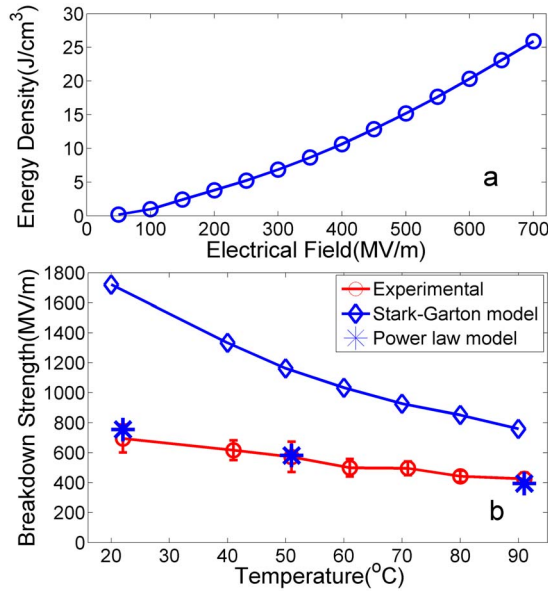


FIG. 1. (Color online) (a) Discharged energy density of P(VDF-HFP) at room temperature. (b) The Weibull breakdown field  $E_b$  as a function of temperature. The predictions on the electromechanical breakdown strength of P(VDF-HFP) at various temperatures based on the Stark-Garton model and power law model are also presented. Data points are shown here and solid curves are drawn to guide eyes. The error bar with experimental data indicates the standard deviation.

a result of the combination of high dielectric constant (see Fig. 2), which is nearly same as that in P(VDF-CTFE) and high breakdown strength. Figure 1(b) presents  $E_b$  as a function of temperature for the P(VDF-HFP) films. In this temperature range,  $E_b$  decreases gradually with temperature and drops from 700 MV/m at room temperature to 425 MV/m at 90 °C. For the films studied, no marked change in  $E_b$  with film thickness was observed. This negative temperature dependence ( $\partial E_b / \partial T < 0$ ) and thickness independence of  $E_b$  suggest that the breakdown be electromechanical in nature, due to the decrease in elastic modulus with temperature, as shown in Fig. 2.<sup>7,9-11</sup>

Electromechanical breakdown is one major breakdown mechanism for insulating polymers, in addition to the electric and thermal breakdown.<sup>7-11</sup> The Stark-Garton model, has been used widely to explain the electromechanical breakdown in polymers.<sup>7-11</sup> Following this model, a polymer of initial thickness  $d_0$  subject to a voltage  $V$  deforms to thickness  $d$ , due to the induced electrostatic stress of  $\frac{1}{2}\epsilon_r\epsilon_0 E^2$ , where  $\epsilon_r$  is the dielectric constant of a polymer. For a linear

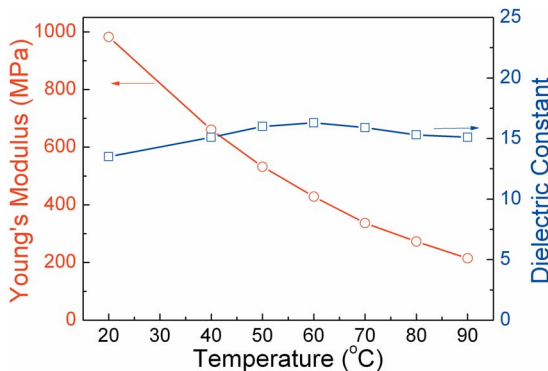


FIG. 2. (Color online) The Young's modulus and dielectric constant at various temperatures for P(VDF-HFP) films.

elastic solid, the mechanical stress is  $Ye$ , where  $Y$  is the Young's modulus and  $e = \ln(d_0/d)$  is the true strain. At equilibrium state, the electrostatic stress is balanced by the mechanical stress, as expressed by

$$\frac{1}{2}\epsilon_r\epsilon_0 E^2 = \frac{1}{2}\epsilon_r\epsilon_0 \left(\frac{V}{d}\right)^2 = Y \ln\left(\frac{d_0}{d}\right). \quad (2)$$

When the function of  $V$  reaches a maximum, the electromechanical instability occurs. This yields the critical true strain and the electromechanical breakdown strength of the polymer,

$$e_c = \ln\left(\frac{d_0}{d_c}\right) = \frac{1}{2}, \quad (3)$$

$$E_c = \frac{V_c}{d_c} = \left(\frac{Y}{\epsilon_r\epsilon_0}\right)^{1/2}, \quad (4)$$

or using the initial thickness  $d_0$ ,  $E_a = E_c(d_c/d_0) = E_c \exp(-1/2)$ .

Combining the Young's modulus and dielectric constant of P(VDF-HFP) shown in Fig. 2, the electromechanical breakdown strength  $E_a$  from the Stark-Garton model is presented in Fig. 1(b). The predicted electromechanical breakdown from Stark-Garton model clearly overestimates the breakdown field strength. In fact, the breakdown strength from the Stark-Garton model is far higher than experimental data for many polymers.<sup>13-15</sup> One reason for this inconsistency is that for many polymers, such as the semicrystalline polymer under consideration in this paper, the Stark-Garton model fails to capture the mechanical properties of the polymer. First, many polymeric materials will not follow the elastic stress-strain relationship of Eq. (2) even at  $d/d_0$  far above 0.6. Moreover, the true strain  $e_c = 0.51$  at breakdown point is not practical and these polymers will experience plastic deformation and mechanical failure at stresses far below  $\sigma_c = Ye_c$  (or electric field far below  $E_c$ ). For better prediction of the critical fields due to electromechanical instability, a model which better characterizes the mechanical behavior of the polymer should be used.<sup>16</sup>

Here, we introduce a more general power law relation to characterize the elastic-plastic deformation of semicrystalline polymers,<sup>17</sup>

$$\sigma = Ke^N = K \left(\log \frac{d_0}{d}\right)^N, \quad (5)$$

where  $K$  scales with the yield strength and  $N$  usually is in the range of 0.1–0.6 for polymers developing plastic deformation.  $N=1$  corresponds to linear elasticity where  $K=Y$ , and  $N=0$  corresponds to ideal plasticity.

Following this formulism, Eq. (2) is modified to

$$\frac{1}{2}\epsilon_r\epsilon_0 \left(\frac{V}{d}\right)^2 = K \left(\log \frac{d_0}{d}\right)^N, \quad (6)$$

which gives

$$E_c = \frac{V}{d_c} = \sqrt{\frac{2K}{\epsilon_r\epsilon_0}} \left(\frac{N}{2}\right)^{N/2}, \quad (7)$$

or using the initial film thickness,  $E_a = E_c d_c / d_0 = E_c \exp(-N/2)$ . Using  $N=1$ , Eq. (7) recovers the Stark-Garton model's prediction of Eq. (4).

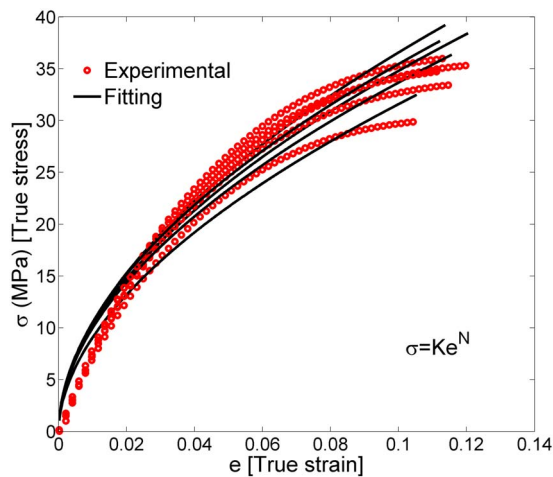


FIG. 3. (Color online) Stress-strain ( $\sigma$ - $e$ ) relation for P(VDF-HFP) films at 22 °C and power law fitting for five samples.

For the approach of Eqs. (5)–(7) to take into account the plastic deformation, the stress-strain behavior for P(VDF-HFP) at room temperature was measured. The data are presented in Fig. 3 along with the fittings of Eq. (5) to the data, yielding the parameters  $K$  and  $N$ , which are presented in Figs. 4(a) and 4(b). It is worth mentioning here that for polymers, the linear elasticity dominates at low strain level ( $N \sim 1$ ). At high strain level when approaching the yielding point, it is the plasticity that dominates instead ( $N \sim 0$ ). This complicated strain-stress behavior does put difficulties in fitting to the experimental data at the whole strain range. However, the key point here is to emphasize the crucial role of plastic deformation on the breakdown strength. Considering this, the model introduced here does capture the overall features and fit the experimental data relatively well. Combining all these results and Eq. (7) yields the electromechanical

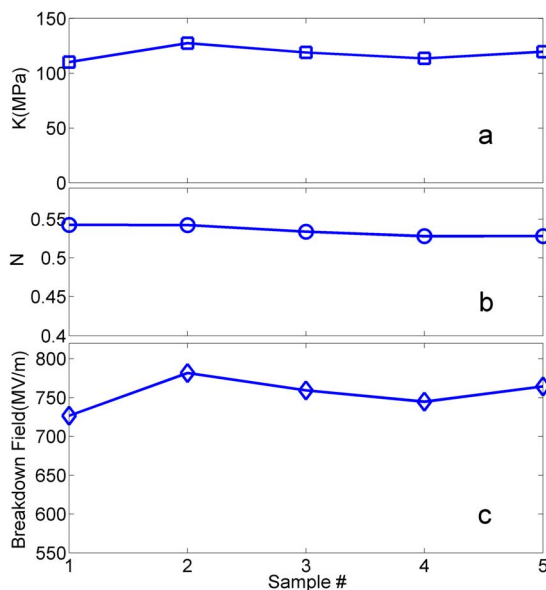


FIG. 4. (Color online) Results of power law fitting to stress-strain curves for P(VDF-HFP) at 22 °C. (a)  $K$ , (b)  $N$ , and (c) calculated breakdown strength using Eq. (7).

breakdown strength  $E_a$  at room temperature, which is presented in Fig. 4(c). As can be seen, the prediction from the power law model ( $\sim 725$ – $780$  MV/m) is in excellent agreement with the experimental data ( $\sim 700$  MV/m). Following the same procedure, the electromechanical breakdown fields from Eq. (7) at 50 and 90 °C were also determined, which yields  $E_a = 581 \pm 4$  MV/m at 50 °C and  $E_a = 394 \pm 3$  MV/m at 90 °C, respectively. These results are presented in Fig. 1(b) and show very good agreement between the model prediction and experimental data for all three temperatures investigated. The results also indicate that the electrical breakdown in these P(VDF-HFP) films is dominated by the electromechanical breakdown.

In summary, we show that by improving the film quality, the breakdown field of P(VDF-HFP) films can reach more than 700 MV/m which leads to a discharged electric energy density higher than 25 J/cm<sup>3</sup>. The experimental results show that the Stark–Garton electromechanical breakdown model significantly overestimates the breakdown strength of the polymer which exhibits plastic deformation at a stress level far below that predicted by the Stark–Garton model. Herein, a more general power law model is introduced to take into account the plastic deformation in the polymers. It is shown that the electromechanical breakdown strength derived based on this approach agrees well with the experimental data for the P(VDF-HFP) copolymer.

The authors from Penn State acknowledge financial support from ONR (Grant No. N00014-05-1-0455) and MURI (Grant No. N00014-05-1-0541). Z.G.S. and X.H.Z. from Harvard University acknowledge financial support from NSF through Project No. CMMI-0800161 on large deformation and instability in soft active materials.

<sup>1</sup>W. J. Sarjeant, J. Zirnheld, and F. W. MacDougall, *IEEE Trans. Plasma Sci.* **26**, 1368 (1998).

<sup>2</sup>H. S. Nalwa, *Handbook of Low and High Dielectric Constant Materials and Their Applications* (Academic, San Diego, 1999).

<sup>3</sup>M. Rabuffi and G. Picci, *IEEE Trans. Plasma Sci.* **30**, 1939 (2002).

<sup>4</sup>J. H. Tortai, N. Bonifaci, A. Denat, and C. Trassy, *J. Appl. Phys.* **97**, 053304 (2005).

<sup>5</sup>B. J. Chu, X. Zhou, K. L. Ren, B. Neese, M. R. Lin, Q. Wang, F. Bauer, and Q. M. Zhang, *Science* **313**, 334 (2006).

<sup>6</sup>X. Zhou, B. J. Chu, B. Neese, M. R. Lin, and Q. M. Zhang, *IEEE Trans. Dielectr. Electr. Insul.* **14**, 1133 (2007).

<sup>7</sup>K. H. Stark and C. G. Garton, *Nature (London)* **176**, 1225 (1955).

<sup>8</sup>J. J. O'Dwyer, *The Theory of Dielectric Breakdown of Solids* (Clarendon, Oxford, 1964).

<sup>9</sup>M. Ieda, *IEEE Trans. Electr. Insul.* **EI-15**, 206 (1980).

<sup>10</sup>L. A. Dissado and J. C. Fothergill, *Electrical Degradation and Breakdown in Polymers* (P. Peregrinus, London, 1992).

<sup>11</sup>K.-C. Kao, *Dielectric Phenomena in Solids* (Academic, Amsterdam, Boston, 2004).

<sup>12</sup>R. Bartnikas and R. M. Eichhorn, *Electrical Properties of Solid Insulating Materials* (American Society for Testing and Materials, Philadelphia, 1983).

<sup>13</sup>J. C. Fothergill, *IEEE Trans. Electr. Insul.* **26**, 1124 (1991).

<sup>14</sup>N. Zebouchi and D. Malec, *J. Appl. Phys.* **83**, 6190 (1998).

<sup>15</sup>J. L. Nash, *Polym. Eng. Sci.* **28**, 862 (1988).

<sup>16</sup>X. H. Zhao, W. Hong, and Z. G. Suo, *Phys. Rev. B* **76**, 134113 (2007).

<sup>17</sup>J. W. Hutchinson and K. W. Neale, *Proceedings of the IUTAM Symposium on Finite Elasticity*, edited by D. E. Carlson and R. T. Shield (Martinus Nijhoff/The Hague, Boston/London, 1979), p. 237.